ELSEVIER

Thermochimica Acta 340–341 (1999) 387–394

thermochimica acta

www.elsevier.com/locate/tca

Apparent kinetic behavior of the thermal decomposition of synthetic malachite

Nobuyoshi Koga[a,*], Jose M. Criado[b], Haruhiko Tanaka[a]

[a]*Faculty of School Education, Chemistry Laboratory, Hiroshima University, 1-1-1 Kagamiyama, Higashi-Hiroshima 739-8524, Japan*

[b]*Instituto de Ciencia de Materiales, CSIC-Universidad de Sevilla, Sevilla 41092, Spain*

Abstract

The influence of self-generated gaseous products on the kinetics and mechanism of the thermal decomposition of synthetic malachite, $Cu_2CO_3(OH)_2$, was investigated by means of conventional TG–DTA under various atmospheric conditions, TG–MS and CRTA under a reduced atmospheric condition, and powder X-ray diffractometry of the partially decomposed sample. It was found that the sample decomposes at a lower temperature under a higher partial pressure of self-generated gases. This interesting behavior, in contrast to the general consideration of chemical equilibrium, results from catalytic action of evolved H_2O on the crystallization of the product CuO, and from an interaction of evolved CO_2 with poorly crystallized CuO under reduced pressure.

Keywords: Kinetics; Thermal decomposition; Synthetic malachite; TG; CRTA; XRD

1. Introduction

The overall kinetics of thermal decomposition of mineral and synthetic copper(II) hydroxide carbonate, i.e., malachite $Cu_2CO_3(OH)_2$, have been reported by many authors [1–12,24]. Malachite is a stable compound formed in the wet corrosion of metallic copper and weathering of such materials. The decomposition of this compound, as is the case with the other basic copper(II) salts, is a possible route to copper(II) oxide with a high surface area. Kinetic modeling of the decomposition process is of interest because it can provide fundamental information on how to control the particle size of the solid product.

It has been reported by many workers that the thermogravimetry for the thermal decomposition of malachite indicates only a smooth mass-loss trace to give copper(II) oxide [1,3–7,9,12,24]: $Cu_2CO_3(OH)_2 \rightarrow 2CuO + CO_2 + H_2O$. Thus, the kinetic analysis of the process has been performed by assuming a single rate process controlled by a rate-limiting step. Recently, Reading and Dollimore [11] reported the results of evolved gas analyses during the thermal decomposition under controlled rate thermal analysis (CRTA) in vacuum, in which the two product gases, CO_2 and H_2O, were not evolved at the same rate during the course of reaction. Interactions of the gaseous products with the solid product at the reaction interface were pointed out as a possible reason for the behavior. This point stimulated our interest in reinvestigating systematically the influence of the self-generated atmosphere on the kinetics.

As the first part of the study, the present paper reports two interesting characteristics of the kinetic

*Corresponding author.

0040-6031/99/$ – see front matter
PII: S0040-6031(99)00289-0

behavior of the decomposition reaction. One is the dependence of decomposition rate on the self-generated gaseous pressures. It has been reported by Henmi et. al.[8] that the DTA peak for the thermal decomposition shifts towards higher temperatures with increasing the partial pressure of CO_2. In contrast, it was found in the present study that the decomposition temperature rises with decreasing partial pressure of the evolved gases. The second kinetic characteristic is the relationship between the two processes, decomposition and crystallization of solid product, and its dependence on the atmospheric condition. Under a reduced pressure ($\sim 10^{-3}$ Pa), the crystalline phase of the solid product, CuO, was not detected by XRD until the fractional decomposition α reaches about 30%. The rate behavior also changed before and after crystallization occurs. It is very probable that the steps of decomposition and crystallization of the solid product take place at different times and separated in space. Characteristics of the present reaction are discussed in connection with these interesting kinetic behaviors.

2. Experimental

Synthetic malachite was prepared by the titration of 1.0 M $CuSO_4$ solution with 1.0 M K_2CO_3 solution [9]. The precipitate produced during the titration was aged, with mechanical stirring, in the mother liquor at 323 K for 2 h. The precipitate was filtered, washed with water and ethanol, and dried in air at 373 K. The product was identified by chemical analysis for Cu^{2+}, FTIR spectroscopy (Shimadzu FTIR8100), X-ray powder diffractometry (XRD; Philips with a Cu target and a monochromator), and TG (Shimadzu TGA-50).

10.0 mg of the sample was weighed into a platinum crucible (2.5 mm in diameter and 5 mm in height). Simultaneous TG–DTA curves at various programmed heating rates β, $1.0 \leq \beta \leq 10.0$ K min^{-1}, were recorded using an ULVAC DTG-9400 instrument with an IR image furnace. The atmospheric condition for the measurements was varied from static air to N_2 flowing at various rates (≤ 90 ml min^{-1}). A series of measurements under reduced pressure (1.5 Pa) were also carried out.

The evolution rates of the gaseous products during the decomposition under a dynamic vacuum were measured by Q-mass spectrometer (VG masstorr 100) equipped with a thermobalance (Cahn 2000). The residual pressure of the balance system was initially reduced to $\sim 10^{-3}$ Pa using a turbomolecular and rotary pumps. Under a dynamic vacuum, the partial pressure of mass number 18 and 44 during the course of reaction were recorded using 5.0 mg of the sample at $\beta = 1.0$ K min^{-1}.

CRTA measurements were performed using an instrument of the Rouquerol type [13,25] constructed with the above thermobalance (Cahn 2000). The residual pressure of the balance system was initially reduced to 2.0×10^{-3} Pa. Under dynamic vacuum with a constant pumping rate, the sample temperature was controlled so as to maintain the atmospheric pressure at 4.0×10^{-3} Pa during the course of reaction. The XRD patterns of the partially decomposed samples during the CRTA measurement with about 100 mg of the sample were recorded after cooling to room temperature.

3. Results and discussion

Fig. 1 shows typical TG–DTG–DTA curves at $\beta = 3.0$ K min^{-1} under flowing N_2 at a rate of 60 ml min^{-1}. Irrespective of the atmospheric conditions applied, the conventional TA curves did not indicate a multi-step reaction, showing only a smooth mass-loss trace. The total mass-loss due to the thermal decompositions, averaged over different atmospheric conditions in the conventional TA measurements, was $28.21 \pm 0.28\%$, being in good agreement with the value of 28.0% calculated by assuming the following reaction: $Cu_2CO_3(OH)_2 \rightarrow 2CuO + CO_2 + H_2O$.

Fig. 2 shows typical TG–MS traces at $\beta =$ 1.0 K min^{-1} under a dynamic vacuum of $\sim 10^{-3}$ Pa. The total mass-loss measured under such a condition was $28.15 \pm 0.21\%$, which supports the above mentioned reaction. In comparison with the decomposition given in Fig. 1, the initial part of the decomposition proceeds at a slower rate under a reduced atmospheric pressure, subsequently accelerated at $\alpha \approx 0.3$. Although both the partial pressure of mass numbers 18 and 44 indicate a peak maximum at around 650 K, the shapes of the peaks are different from each other, indicating that the two gaseous products are evolved at different rates throughout the decomposi-

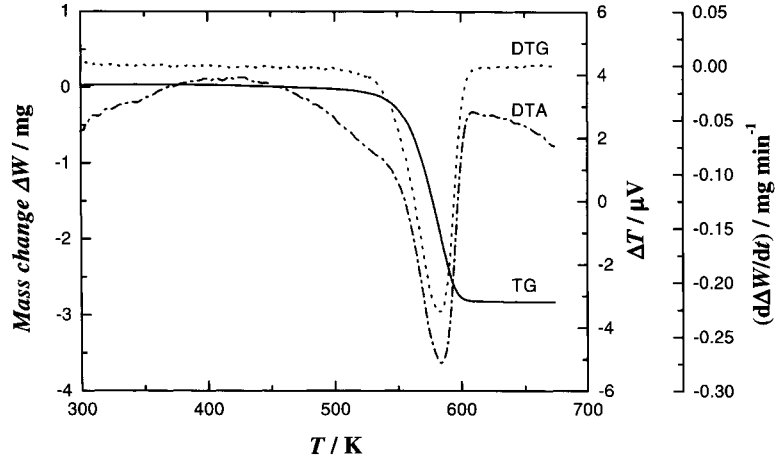

Fig. 1. Typical TG–DTG–DTA traces at $\beta = 3.0$ K min^{-1} under flowing N_2 at a rate of 60 ml min^{-1}.

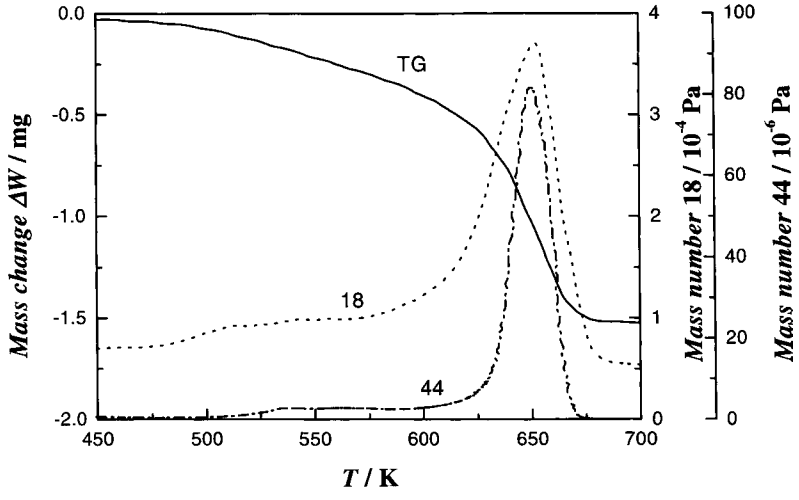

Fig. 2. Typical TG–MS traces at $\beta = 1.0$ K min^{-1} under a dynamic vacuum of $\sim 10^{-3}$ Pa.

tion. At the early stage of the reaction, the evolution rate of water vapor is higher than that of carbon dioxide. A sharper peak was observed for the evolution rate of CO_2 than that of H_2O. This behavior is in good agreement with the CRTA data under reduced pressure reported by Reading and Dollimore [11], and is inconsistent with the above assumption of a single rate process. It is also interesting to compare the present result with the TG–MS data under flowing He reported by Brown et al. [6], where the two gases are evolved at approximately the same rate during the course of reaction. This disagreement indicates the possibility of a change in the decomposition process that depends on the atmospheric conditions, including the self-generated atmosphere.

Fig. 3 shows the influence of the atmospheric conditions on the kinetic rate data obtained from conventional nonisothermal TG at $\beta = 3.0$ K min^{-1}. As the partial pressure of the evolved gases is decreased by increasing the flow rate of N_2 and by reducing the total pressure, the kinetic curves shift to the higher temperature region. This behavior contrasts with the general trend of the thermal decomposition of solids, deduced from considerations based on chemi-

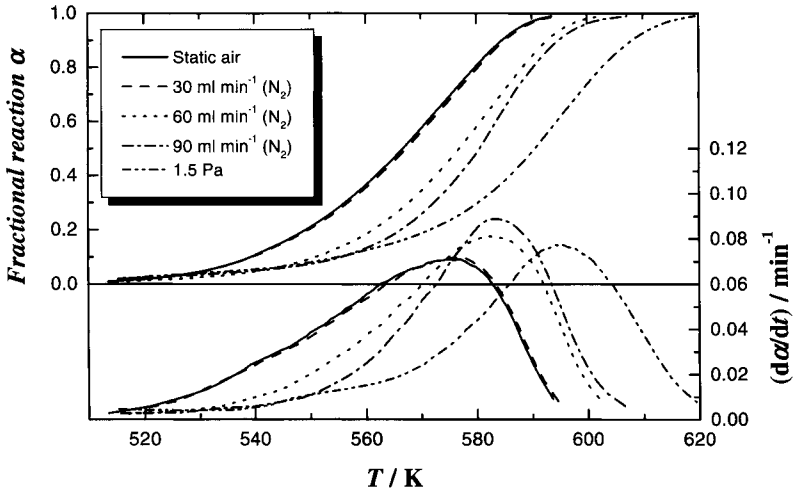

Fig. 3. The influence of atmospheric conditions on the kinetic rate data at $\beta = 3.0$ K min^{-1}.

cal equilibrium. It is also apparent that the induction period of the decomposition increases with decreasing the partial pressure of the evolved gases.

From a series of conventional TG curves at different β, apparent activation energies, E, for the thermal decomposition under various atmospheric conditions were obtained by the Friedman method [14].

$$\ln\frac{d\alpha}{dt} = -\frac{E}{RT} + \ln[Af(\alpha)], \quad (1)$$

where $f(\alpha)$ is the kinetic model function listed elsewhere [15–18]. By plotting $\ln(d\alpha/dt)$ against T^{-1} at a selected α, the value of E can be obtained from the slope. Fig. 4 shows the Friedman plots for the process under different atmospheric conditions and at various α. Over the initial part of the reaction, see Fig. 4(a), the slope of the plot decreases gradually with increasing the partial pressure of the evolved gases. Similar behavior was observed until around $\alpha = 0.3$. In the subsequent process, the slopes of the Friedman plots

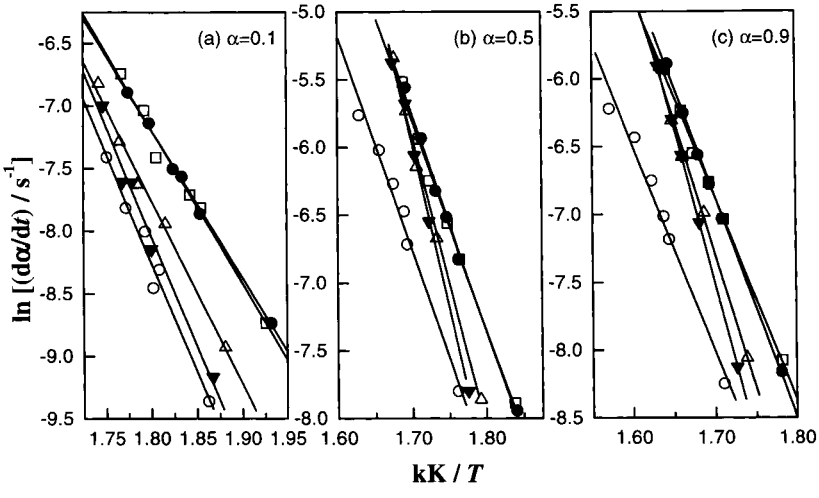

Fig. 4. Comparison of the Friedman plots for the processes under different atmospheric conditions:(□) static air, (●) N_2 flowing at 30 ml min^{-1}, (△) N_2 flowing at 60 ml min^{-1}, (▼) N_2 flowing at 90 ml min^{-1}, and (○) reduced pressure of 1.5 Pa.

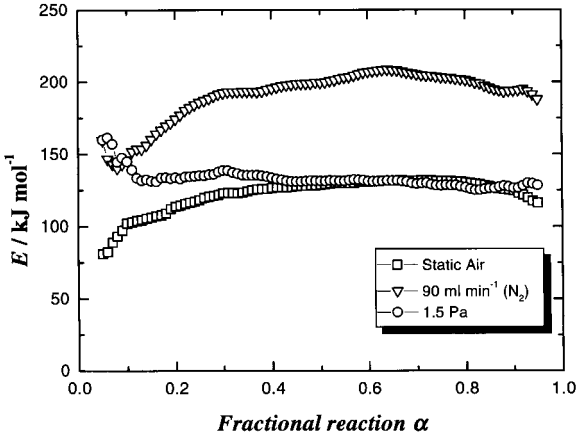

Fig. 5. Comparison of the dependence of the apparent value of E on α under different atmospheric conditions.

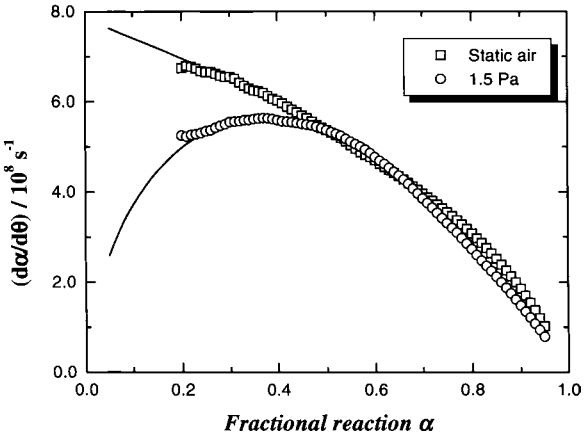

Fig. 6. Comparison of plots of $d\alpha/d\theta$ against α for the processes under static air and under a reduced pressure of 1.5 Pa.

for the reactions under a static atmosphere and under reduced pressure are identical. The change in the slope of the Friedman plots for the reactions under flowing N_2 seems to result from a change in the influence of the evolved gases which depends on the heating rate applied, because the data points at lower and higher β are positioned close to those obtained under reduced pressure and under static air, respectively.

In Fig. 5, the dependence of apparent values of E on α determined under different atmospheric conditions is compared. The E values for the process under flowing N_2 at a rate of 90 ml min^{-1} are in good agreement with those reported by Reading and Dollimore [11]. It is apparent from Fig. 4, however, that the influence of the self-generated gaseous pressure changes depending on the heating rate for the process under flowing N_2. Thus the values of E determined nonisothermally under flowing N_2 are less meaningful for describing the kinetics of the process. For the process under reduced pressure, a nearly constant value of E was obtained in the range $0.20 \leq \alpha \leq 0.95$ with a mean value of 131.3 ± 0.4 kJ mol^{-1}. Under static air, the value of E increases gradually and reaches a constant value at $\alpha \geq 0.4$, that is identical with the value obtained under reduced pressure. This implies that, in such a range of α, the influence of the self-generated gaseous atmosphere on the kinetic behavior appears only as a certain α-dependent function, irrespective of the rate data under static air and under reduced pressure. Because all the α-dependent functions in the kinetic equation are eliminated in the Friedman method [19,20,26,27], an identical value of E is obtained under static air and under reduced pressure.

Using the values of E obtained at respective α, the rate data measured under static air and under reduced pressure were extrapolated to infinite temperature according to the following equation [21–23,28,29]:

$$\frac{d\alpha}{d\theta} = \frac{d\alpha}{dt}\exp\left(\frac{E}{RT}\right), \tag{2}$$

where θ is the generalized time proposed by Ozawa [21,28,29]. Fig. 6 compares the plots of $d\alpha/d\theta$ against α plots for the processes under static air and under reduced pressure. The major difference between the two rate behaviors is seen in the range $\alpha \leq 0.5$. The overall rate behavior under static air is predominantly deceleratory. On the other hand, a peak maximum at $\alpha = 0.37$ was observed for the process under reduced pressure. The value of $d\alpha/d\theta$ can be expressed by [21–23,28,29],

$$\frac{d\alpha}{d\theta} = Af(\alpha). \tag{3}$$

An appropriate $f(\alpha)$, for describing the overall reaction behavior within $0.20 \leq \alpha \leq 0.95$, was determined through plotting various $f(\alpha)$ against $d\alpha/d\theta$. Table 1 lists the most appropriate $f(\alpha)$ for the processes under static air and under reduced pressure, together with the apparent pre-exponential factor, A, calculated from the slope of a plot of $f(\alpha)$ against $d\alpha/d\theta$. Different kinetic models, phase boundary controlled (R_n) and

Table 1
The most appropriate $f(\alpha)$ for the processes under static air and under reduced pressure, together with the apparent value of A determined from the $f(\alpha)$ vs. $d\alpha/d\theta$ plots

Atmosphere	$f(\alpha)$	Exponent	ln(A) (s^{-1})	γ^a
Static air	$n(1-\alpha)^{1-1/n}$	$n = 1.8$	20.1 ± 0.1	0.9988
1.5 Pa	$m(1-\alpha)[-\ln(1-\alpha)]^{1-1/m}$	$m = 1.8$	20.3 ± 0.1	0.9987

[a] Correlation coefficient of the linear regression analysis of the plot of $f(\alpha)$ against $d\alpha/d\theta$.

Avrami–Erofeev (A_m), were found to characterize the overall kinetic behavior under static air and under reduced pressure, respectively. In Fig. 6, the theoretical curves drawn by assuming the apparent kinetic model and value of A listed in Table 1 are shown, indicating the fairly good agreement to the data points. It seems that the difference results from the change in the reaction behavior at the early stage of the reaction that is influenced by the atmospheric conditions.

Fig. 7 shows a typical CRTA record obtained under dynamic vacuum using 10.75 mg of the sample. The temperature profile during the reaction changes at around $\alpha = 0.3$, showing similar behavior in the early stage of reaction to the other results obtained under reduced pressure. Reading and Dollimore [11] reported that the surface area of the sample, decomposed under reduced pressure, increases dramatically over the early stage of the reaction. Changes in the XRD pattern during the CRTA measurement under reduced pressure, using about 100 mg of the sample, are shown in Fig. 8. No peak corresponding to CuO can be seen in the range $\alpha \leq 0.3$. This experimental evidence indicates that, under reduced pressure, crystallization of the decomposition product CuO occurs with difficulty over the early stage of the reaction. Consequently, the steps of decomposition and crystallization of the solid product take place at different times and separated in space. Some interaction between the poorly crystallized CuO and evolved CO_2 seems to be a probable reason for the slower rate of CO_2 evolution than H_2O over the early stage of reaction.

It is seen from Fig. 3 that such behavior during the early stage of reaction gradually disappears with increasing partial pressure of the evolved gases. Because the DTA peak for the thermal decomposition shifts to higher temperature with increasing partial pressure of CO_2 [8], it seems that the reaction is accelerated by the higher water vapor pressure generated by the reaction itself. Catalytic action of the

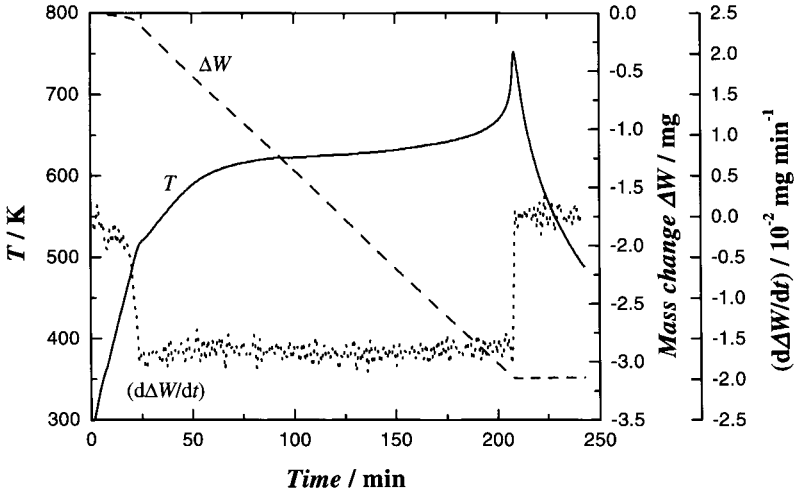

Fig. 7. A typical CRTA record of a 10.75 mg sample under a controlled residual pressure of 4.0×10^{-3}Pa.

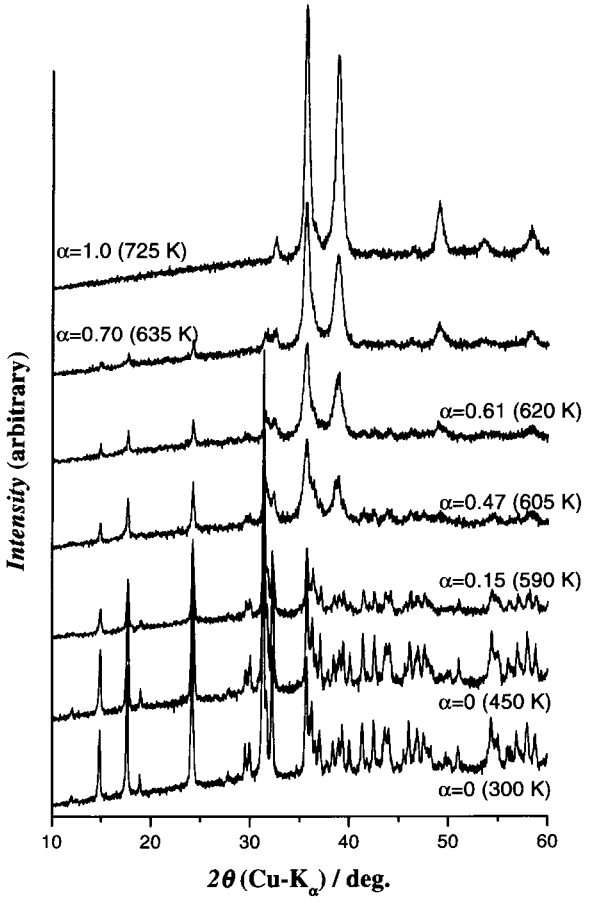

Fig. 8. Typical XRD patterns of the partially decomposed samples in the CRTA under the controlled residual pressure of 4.0×10^{-3} Pa.

water vapor on the crystallization of CuO is one probable reason for the higher reactivity of the sample under higher partial pressures of evolved gases. From the above experimental evidence, it is apparent that the kinetic characterization of the decomposition requires very complicated considerations concerning the chemical equilibrium of the reactant solid with the product gases, catalytic action of evolved water vapor on the crystallization of CuO, an interaction of evolved CO_2 with poorly crystalline CuO, and so on. A more quantitative characterization of the kinetics and mechanism of the thermal decomposition of synthetic malachite by means of CRTA measurements under various controlled atmospheres will be reported elsewhere.

4. Conclusion

Two interesting characteristics of the decomposition behavior of synthetic malachite were identified by examining the influence of self-generated atmospheric conditions on the course of reaction.

1. Under reduced pressure conditions, two product gases, H_2O and CO_2, are evolved at different rates during the course of reaction.
2. The higher rates of decomposition are observed under higher partial pressures of self-generated gases.

The decomposition proceeds in a very complicated way that is influenced by the chemical equilibrium of the solid product and gaseous products, a catalytic action of evolved H_2O for the crystallization of CuO, and an interaction of evolved CO_2 with the poorly crystallized CuO. Assumption of a single rate process for kinetic analysis, which has been employed in the former kinetic studies of the present reaction, is applicable only within a restricted range of experimental conditions, because the rate behavior changes by the effect of the self-generated atmospheric conditions.

References

[1] P. Ramamurthy, E.A. Secco, Can. J. Chem. 48 (1970) 3510.
[2] M.K. Seguin, Can. Mineral 13 (1975) 127.
[3] J. Morgan, J. Thermal Anal. 12 (1977) 245.
[4] Z.D. Zivkovic, D.F. Bogosavljevic, V.D. Zlatkovic, Thermochim. Acta 18 (1977) 235, 310.
[5] D. Dollimore, T.J. Taylor, Thermochim. Acta 40 (1980) 297.
[6] I.W.M. Brown, K.J.D. Mackenzie, G.J. Gainsford, Thermochim. Acta 74 (1984) 23.
[7] I.M. Uzunov, D.G. Klissurski, Thermochim. Acta 81 (1984) 353.
[8] H. Henmi, T. Hirayama, N. Mizutani, M. Kato, Thermochim. Acta 96 (1985) 145.
[9] H. Tanaka, Y. Yamane, J. Thermal Anal. 38 (1992) 627.
[10] S.A.A. Mansour, J. Thermal Anal. 42 (1994) 1251.
[11] M. Reading, D. Dollimore, Thermochim. Acta 240 (1994) 117.
[12] N. Koga, Thermochim. Acta 258 (1995) 145.
[13] J. Rouquerol, J. Thermal Anal. 2 (1970) 123.
[14] H.L. Friedman, J. Polym. Sci. Part C 6 (1964) 183.
[15] S.F. Hulbert, J. Br. Ceram. Soc. 6 (1969) 11.
[16] M.E. Brown, D. Dollimore, A.K. Galwey, Reactions in the Solid State, Elsevier, Amsterdam, 1980.
[17] J. Sestak, Thermophysical Properties of Solids, Elsevier, Amsterdam, 1984.

[18] H. Tanaka, N. Koga, A.K. Galwey, J. Chem. Educ. 72 (1995) 251.
[19] N. Koga, J. Thermal Anal. 49 (1997) 45.
[20] N. Koga, J.M. Criado, J. Thermal Anal. 49 (1997) 1477.
[21] T. Ozawa, Bull. Chem. Soc. Jpn. 38 (1965) 1881.
[22] J. Malek, Thermochim. Acta 200 (1992) 257.
[23] N. Koga, J. Malek, J. Sestak, H. Tanaka, Netsu Sokutei 20 (1993) 210.
[24] D. Dollimore, T.J. Taylor, in: Proceedings of the Seventh ICTA, Ontario, 1982, p. 636.
[25] J. Rouquerol, J. Thermal Anal. 5 (1973) 203.
[26] N. Koga, J.M. Criado, J. Am. Cer. Soc. 81 (1998) 2901.
[27] N. Koga, J.M. Criado, Int. J. Chem. Kinet. 30 (1998) 737.
[28] T. Ozawa, J. Thermal Anal. 2 (1970) 301.
[29] T. Ozawa, J. Thermal Anal. 31 (1986) 547.